https://doi.org/10.1016/j.engstruct.2017.04.007

Typhoon- and Temperature-induced Quasi-static Responses of A Supertall Structure

J.Z. Su[a,b], Y. Xia[b,*], L.D. Zhu[c], H.P. Zhu[d], Y.Q. Ni[b]

[a]*College of Civil Engineering, Fuzhou University, Fuzhou, China*

[b]*Department of Civil and Environmental Engineering, The Hong Kong Polytechnic University, Hung Hom, Kowloon, Hong Kong*

[c]*State Key Laboratory of Disaster Reduction in Civil Engineering, Tongji University, Shanghai, China*

[d]*School of Civil Engineering and Mechanics, Huazhong University of Science and Technology, Wuhan, China*

[*]Corresponding author: ceyxia@polyu.edu.hk

ABSTRACT

Wind loads and the associated load effects on supertall structures are key factors in structural design. In practice, typhoon-induced quasi-static responses measured from the field mix with temperature-induced responses because temperature varies significantly during a typhoon event. The mixed responses complicate the assessment of the wind loading effects and the separation of the two load effects is difficult in practice. In this study, the wind- and temperature-induced quasi-static responses of the 600 m-tall Canton Tower are investigated using a comprehensive long-term structural monitoring system installed on the structure. The structural responses (stresses and displacement) obtained from the field monitoring system during a strong typhoon are presented. The temperature-induced responses are calculated by applying a temperature loading model to the finite element model of the structure. The purely typhoon-induced quasi-static responses are then separated from the total measured responses by subtracting the temperature-induced ones. It shows that the typhoon-induced quasi-static responses of the supertall structure are slightly smaller than the temperature-induced responses in a typical sunny day. The typhoon-induced quasi-static displacement obtained from the field is also compared with the counterpart from the wind tunnel test on an aeroelastic model of the full tower.

Keywords: supertall structure, temperature effect, wind effect, field monitoring, quasi-static response

1. Introduction

Wind load is critical to supertall structures located in coastal cities that are frequently subjected to typhoons. The wind speed can be generally decomposed as a mean component and turbulence components, which cause the mean and dynamic responses of the structure, respectively. Supertall structures are prone to large mean and dynamic wind-induced responses because of low natural frequencies and small structural damping. The wind effect is a governing factor in designing supertall structures.

Wind tunnel tests on scale models of structures and their surroundings are widely employed to identify wind loads and associated structural responses. [1-3]. Specifically, aerodynamic/ aeroelastic models are used to investigate the characteristics of wind pressure and forces in the time and frequency domains acting on high-rise structures with various cross-sections [4-7]. Aerodynamic parameters obtained from wind tunnel tests have been adopted for structural analysis or design [8].

The recently developed field monitoring exercises of supertall structures under strong winds usually focuses on measuring wind speed and direction through anemometers, wind pressure through pressure sensors, and wind-induced mean and dynamic structural responses through accelerometers and global positioning system (GPS) [9-11]. The wind-induced responses of a 233.9 m-high 66-story high-rise building were measured [12]. The 10−min horizontal displacement of the structure was measured of −11.7 to 20.9 mm and mean of 3.0 mm in one direction and 31.8 to 61 mm and mean of 44.0 mm in the other perpendicular direction. The mean wind speed on the tower top was 12.29 m/s with a prevalent wind direction of 260° [12].

High-rise structures are also subject to daily, seasonal, and yearly environmental temperature effects induced by varying solar radiation and ambient air temperature [13]. Temperature variations in structural components will cause movement and usually lead to thermal stress. Unlike those on bridges [14, 15], studies on the temperature action of supertall structures are limited because of insufficient real measurement data. In the past decades, investigations of tall buildings are limited due to the uniqueness of the construction site and structural configuration. Since the 1970s, temperature effects on tall TV towers [16, 17], and a steel towers [18] have been analyzed. A small number of research works have focused on temperature effects on tall structures at the construction stage [19, 20].

Typhoons typically occur for one or two days in summer, during which the air temperature decreases significantly but slowly. In field monitoring exercises, the measured structural responses during a typhoon period include the mean response and dynamic response. The latter can be easily separated from the former as they have different frequency components. The former itself (mean response) contains the mean wind effect and temperature effect, both varying in a similar time scale, for example, hourly. The associated structural mean responses are referred to as quasi-static responses hereinafter and only the quasi-static responses will be studied in the present paper unless specified. In practice, separating the quasi-static responses due to the mean wind effect and temperature effect directly from the measurement data is difficult. Finding other periods with a similar temperature decrease without strong wind in summer is difficult. Alternatively, the temperature effects may be eliminated by calculating the temperature-induced responses during a typhoon period. This calculation requires the temperature distribution of the structure during the typhoon period be available.

The typhoon-induced quasi-static responses of the 600 m-tall Canton Tower will be investigated in this study, with emphasis on the separation of temperature effects. The supertall structure is located in Guangzhou, a strong typhoon-prone region in the south of China. Given its complicated spatial configuration, measuring or calculating the wind loading of the entire structure is difficult. A wind tunnel test was carried out on an aeroelastic model of the structure in the Boundary Layer Wind Tunnel at Tongji University to investigate the quasi-static and dynamic responses of the structure to turbulent winds [21].

A comprehensive long-term structural health monitoring (SHM) system has been installed on Canton Tower to improve understanding of various loading environment and effects (e.g., temperature fluctuation, strong winds, and earthquakes) during the construction and service stages [22, 23]. In this study, the structural responses (displacement and stresses) before and during one strong typhoon are presented first. The temperature-induced quasi-static responses are then calculated from a finite element (FE) model with the verified temperature distribution of the structure [23]. The typhoon-induced quasi-static responses are subsequently obtained by subtracting the temperature effects. Finally, the calculated wind responses are compared with the wind tunnel test results under the measured wind direction and speed. It is noted that varying temperature has an effect on the material mechanical properties such as Young's modulus and then on the vibration properties of the structure such as frequencies [24, 25]. The effect is not significant and will not be included in this study.

2. Canton Tower

The 600 m-high Canton Tower is a typical tube-in-tube supertall structure (Figure 1). The 454 m-high main tower consists of a reinforced concrete inner tube with a constant 14 × 17 m oval and a steel outer tube whose cross-section varies and rotates along the height. A total of 37 functional floors and four levels of connection girders link the inner tube to the outer tube. The floors serve various functions, including TV and radio signal transmission facilities, open-air skywalk, offices, and entertainment facilities. The 146 m-high spatial steel antenna is located on the top of the main tower. This special exterior geometry results in the structural behavior complicated, particularly under winds.

A comprehensive long-term SHM system has been established in the structure for integrated in-construction and in-service monitoring. The monitoring system was installed gradually as the construction of the structure progressed. A weather station, an anemometer, and a GPS system have been installed at the main tower top. Numerous strain gauges and temperature sensors have also been installed at four façades of the inner and outer tubes at 12 different elevations to measure the static strain and temperature of the structure. Ni et al. [22] provided detailed descriptions of the SHM system. Xia et al. [26] reported the strain monitoring of the structure during the construction stage, and Su et al. [23] studied the temperature distribution of the structure during the service stage.

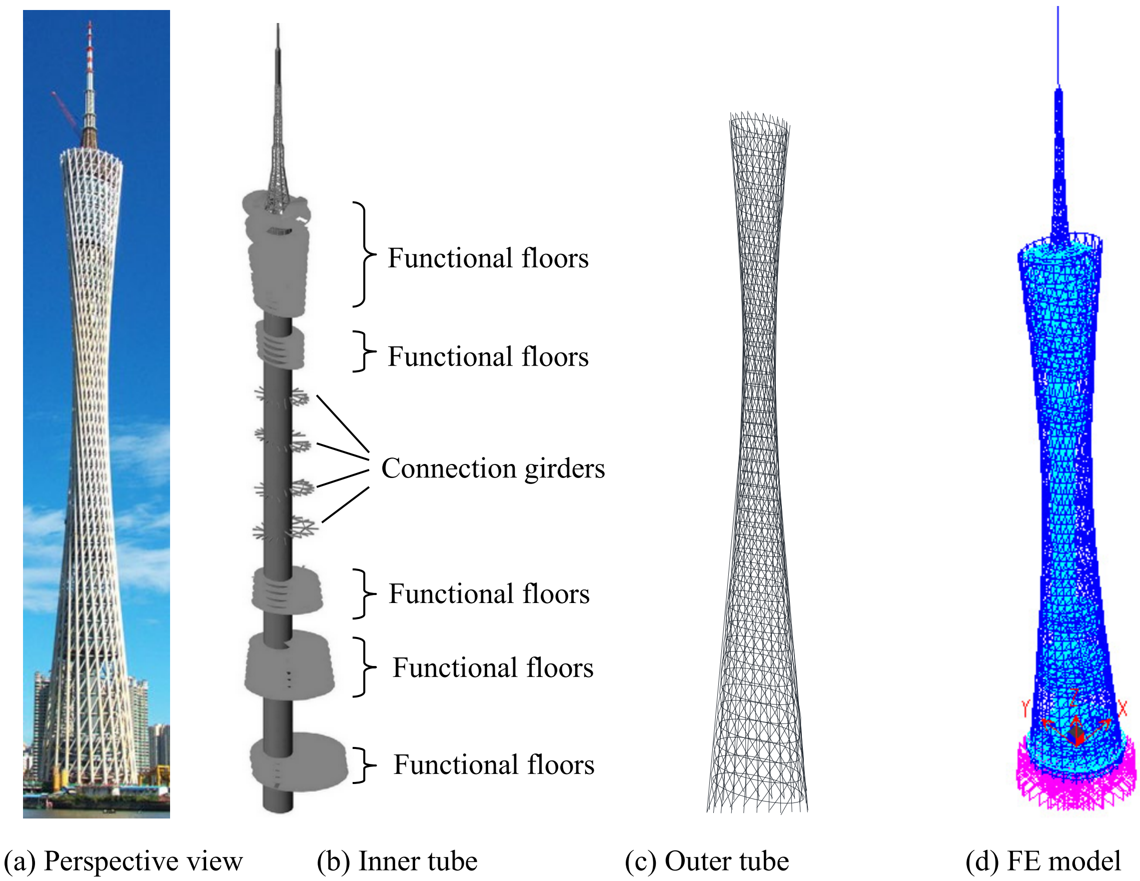

Figure 1. Canton Tower

A global FE model of the Canton Tower has been constructed using the general FE software package SAP2000 [27] (Figure 1(d)), to calculate the temperature-induced displacement and stress responses. In this model, four-node and three-node area elements with six degrees of freedom (DOFs) at each node are employed for the shear walls of the inner tube and the floor decks. Two-node 3D beam elements with six DOFs at each node are used to model the outer tube members, the connection girders between the inner and outer tubes, and the antenna mast. All nodes in the basement are fixed in all directions. The full model contains 43,067 elements and 28,305 nodes. The first 14 vibrational frequencies are calculated below 1.5 Hz [28]. The first two mode shapes are of flexural type along two perpendicular directions of the inner tube with the frequency of 0.095 Hz and 0.139 Hz.

3. Quasi-static Responses of Canton Tower from Field Monitoring

3.1. Meteorological data during typhoon period

Typhoon Usagi, a strong tropical cyclone that struck Guangdong Province from 22 to 23 September, 2013, is selected to investigate the wind-induced quasi-static responses of Canton Tower. The typhoon moved west-northwest across the Luzon Strait on 21 September and across the northeastern part of the South China Sea on 22 September, landing near Guangzhou in the evening. The track of the storm is shown in Figure 2.

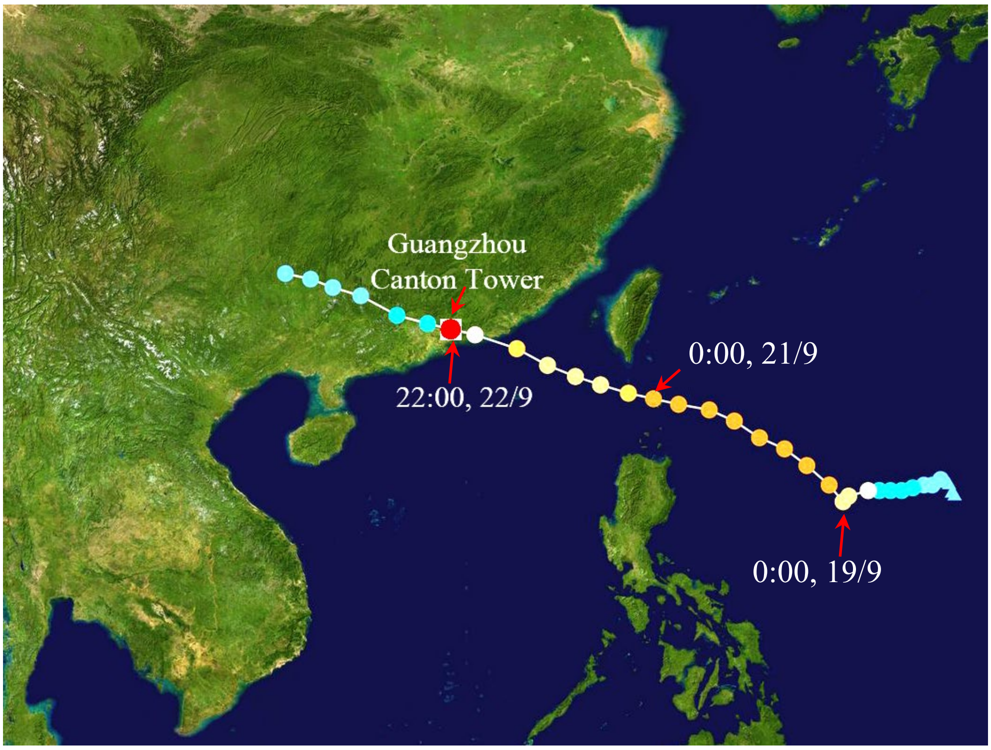

Figure 2. Trail of Typhoon Usagi

Figure 3 illustrates the 10−min mean wind speed and wind direction on 21 to 23 September, as measured by the anemometer installed at the top of the main tower. From 0:00 to 24:00 on 21 September, the wind speed was no more than 9.0 m/s, which was considered a non-typhoon period. The mean wind speed increased to 12.0 m/s at 14:00 on 22 September as the typhoon approached. The speed continued to grow to approximately 18 m/s at 19:00 on 22 September, reaching a maximum of 25.0 m/s at 4:00 on 23 September. The wind speed then decreased to 8.0 m/s as the typhoon continued to move landward. The wind direction was mainly from the north on 21–22 September and turned to the northwest from 0:00 to 4:00 on 23 September, and southwest from 4:00 to 8:00.

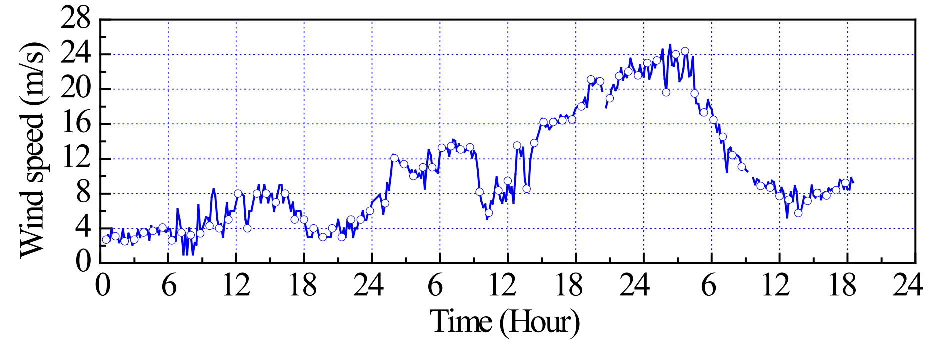

(a)

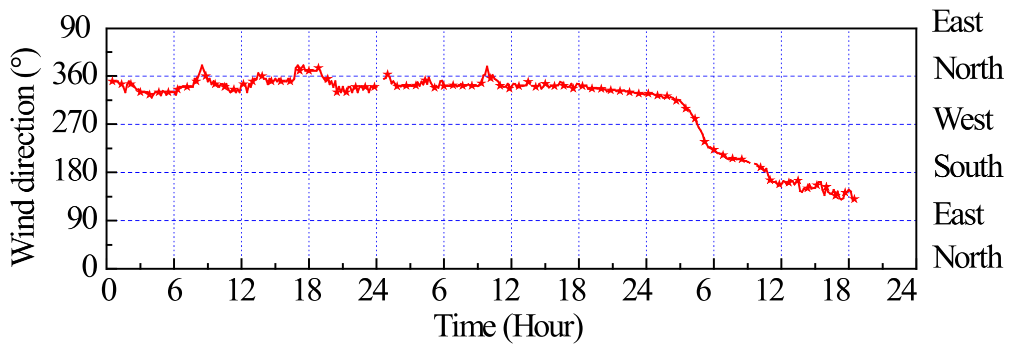

(b)

Figure 3. Ten-minute mean wind speed and direction at the top of the main tower on 21-23 September 2013

The air temperature during these three days is illustrated in Figure 4. 21 September was a typical sunny summer day with an air temperature variation of 25.5–31.0 °C and no strong wind. Air temperature then decreased as the typhoon gradually approached. The average air temperature during the typhoon period (from 12:00 on 22 to 12:00 on 23 September) was 4.0 °C lower than that during the non-typhoon period (from 0:00 to 24:00 on 21 September. The structural quasi-static responses during the typhoon period were mainly induced by the combination of temperature changes and mean wind. The two effects must be separated such that those caused by the typhoon solely can be evaluated.

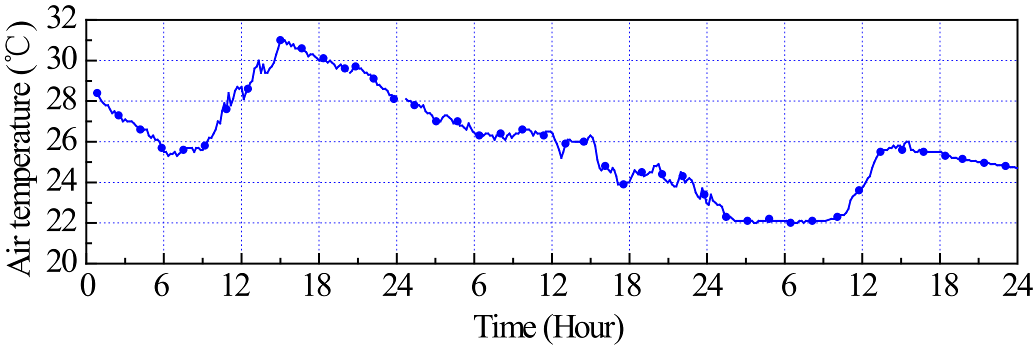

Figure 4. Air temperature at the top of the main tower on21-23 September, 2013

3.2. Structural displacement

Figure 5 presents the GPS-measured horizontal displacement at the tower top from 21-23 September at ten minute intervals, with the initial position as the origin point. The data were averaged every 10 min period. The displacement track is illustrated in Figure 6. The tower moved relatively slow before sunrise on 21 September, moving to the west after sunrise and arriving at its westernmost position at approximately 10:00. This movement is attributed to the sun rising from the east in the morning. The tower members in the east had higher temperature than those in the west; thus, the structure bent away from the sun. For the same reason, the tower moved toward the northeast in the afternoon and reached its northernmost position at approximately 17:30. After sunset, the temperature difference between the tower members decreased. The tower gradually moved back from the north to the south and finally returned to the initial point at 24:00. The peak-to-peak motion throughout the day was 17.8 and 8.5 cm in the east-west and south-north direction, respectively.

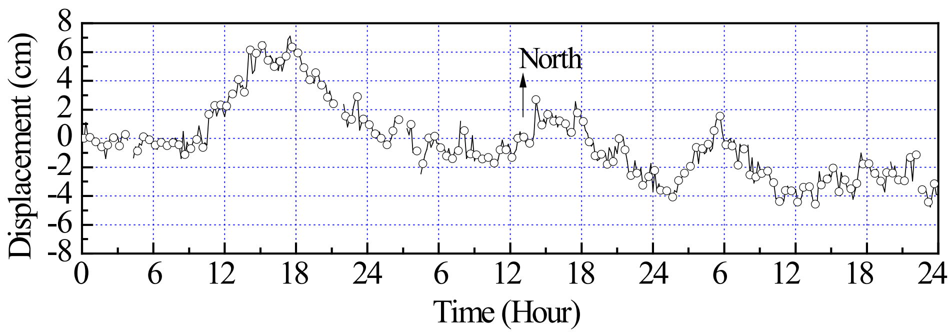

(a) North-south direction

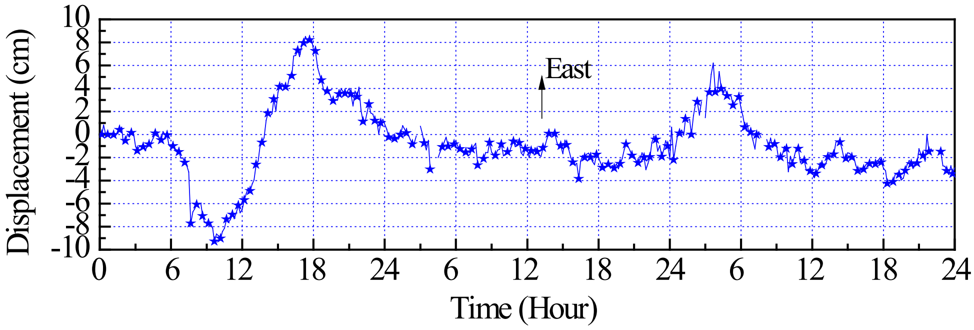

(b) East-west direction

Figure 5. Horizontal displacement at the tower top on 21-23 September 2013

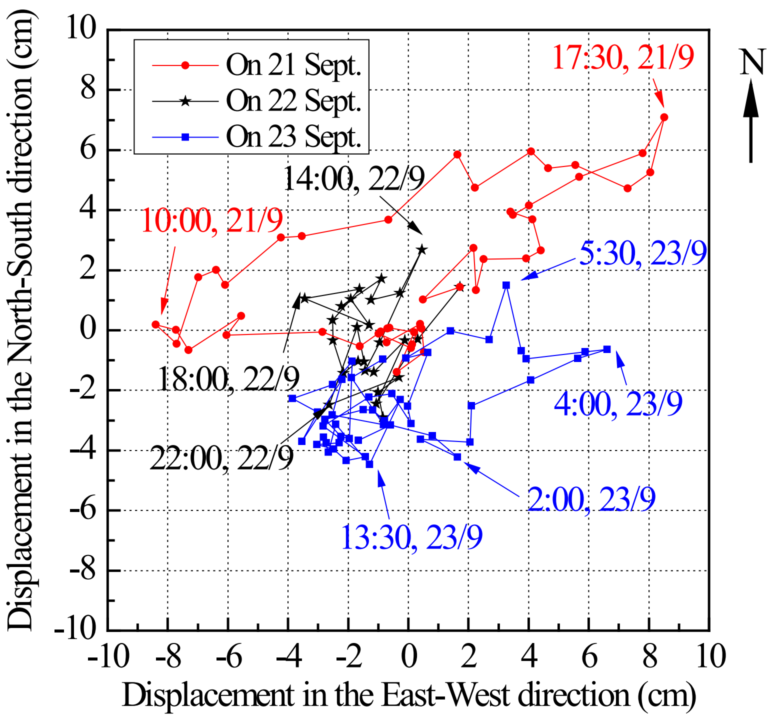

Figure 6. Displacement track at the tower top on 21-23 September 2013

Subsequently, the tower top moved to the south by approximately 7.0 cm from 14:00 on 22 September to 2:00 on 23 September, with the increasing north wind. It then leaned toward the northeast by approximately 6.2 cm from 2:00 to 4:00 on 23 September with the maximum west-northwest wind. Afterward, the tower top returned toward the west as wind speed slowed down from 4:00 to 8:00 on 23 September. The peak-to-peak motion during the typhoon period was roughly 10.1 and 7.0 cm in the east-west and north-south direction, respectively (Figure 6).

3.3. Structural stresses

The stress of the reinforced concrete core wall of the inner tube was mainly in the vertical direction. The vertical stress (σ) was calculated from the measured vertical strain by eliminating the free thermal expansion as $\sigma = E(\varepsilon - \alpha_T \Delta T)$, where E is Young's modulus of material, ε is the measured total strain, α_T is the thermal coefficient of linear expansion of the material, and ΔT is the temperature change.

Figure 7 shows the vertical stresses of the four façades of the inner tube at an elevation of 303.2 m, from 21 to 23 September 2013. The data were averaged every 10 min period. The stress in this study is the total stress of the structure, including that caused by the dead load.

21 September was a sunny day with 4.8 m/s mean wind speed. The variation of the stress within the day was mainly induced by temperature variations. The vertical stresses remained stable in the early morning and then increased (compression decreased) as the structural temperature increased. In the afternoon, the stress decreased and returned to the initial value in the evening and at midnight. Stresses of the various façades reached their maximum at different time instants. The east façade was under maximum stress at approximately 12:00. The south wall reached maximum at around 16:00, followed soon after by the west wall. As expected, the stress variation on the north side was the smallest (approximately 0.3 MPa), whereas that on the west was the largest at approximately 0.7 MPa. During daytime, all inner tubes were subjected to tension, unlike during early morning. This is because although the entire structure experienced a temperature increase during daytime, the outer tube had a larger temperature increase than the inner tube, causing the former to experience larger vertical expansion than the latter. Consequently the inner tube was in tension, whereas the outer tube was in compression. Su et al. [23] investigated the stress redistribution of the entire structure in detail.

On 22 September, the stress of the inner tube at an elevation of 303.2 m remained stable until 12:00. The stress began to fluctuate significantly from 18:00 to 10:00 on 23 September, when the typhoon weakened. During the period, all façades were subjected to compressive stresses, except the west. The north façade had the largest compressive stress of approximately −0.5 MPa, while the west was under a tensile stress of 0.4 MPa. The effects of the typhoon on the structure differed from those of the temperature.

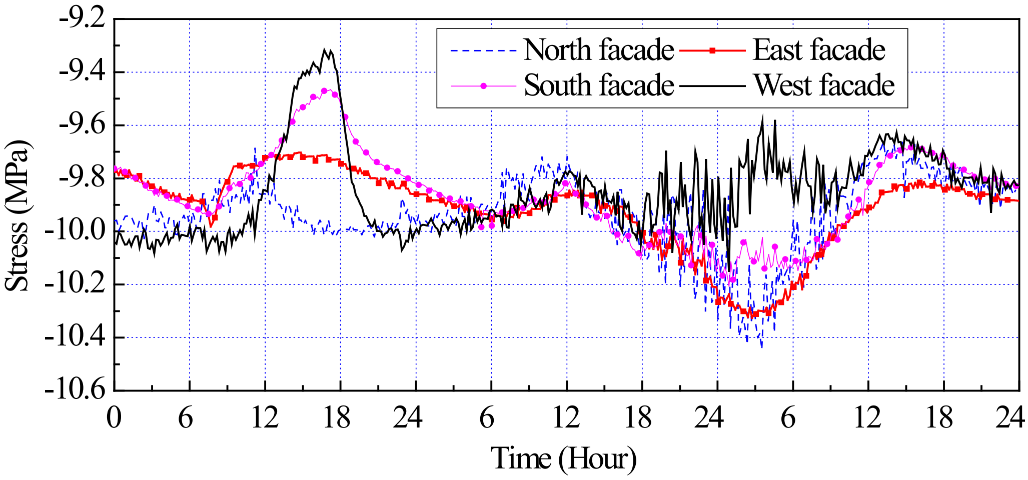

Figure 7. Vertical stress of the inner tube 21-23 September 2013

Changes in the vertical stresses of the inner tube on different sections of the tower are compared in Figure 8 to illustrate the typhoon-induced quasi-static responses at various heights of the tower. Excluding the west façade, which was under tension, the north, east, and south façades of all sections were under compression during the typhoon period. The maximum typhoon-induced stress (0.55 MPa), accounting for 5.5% of the total stress, occurred at Section 3.

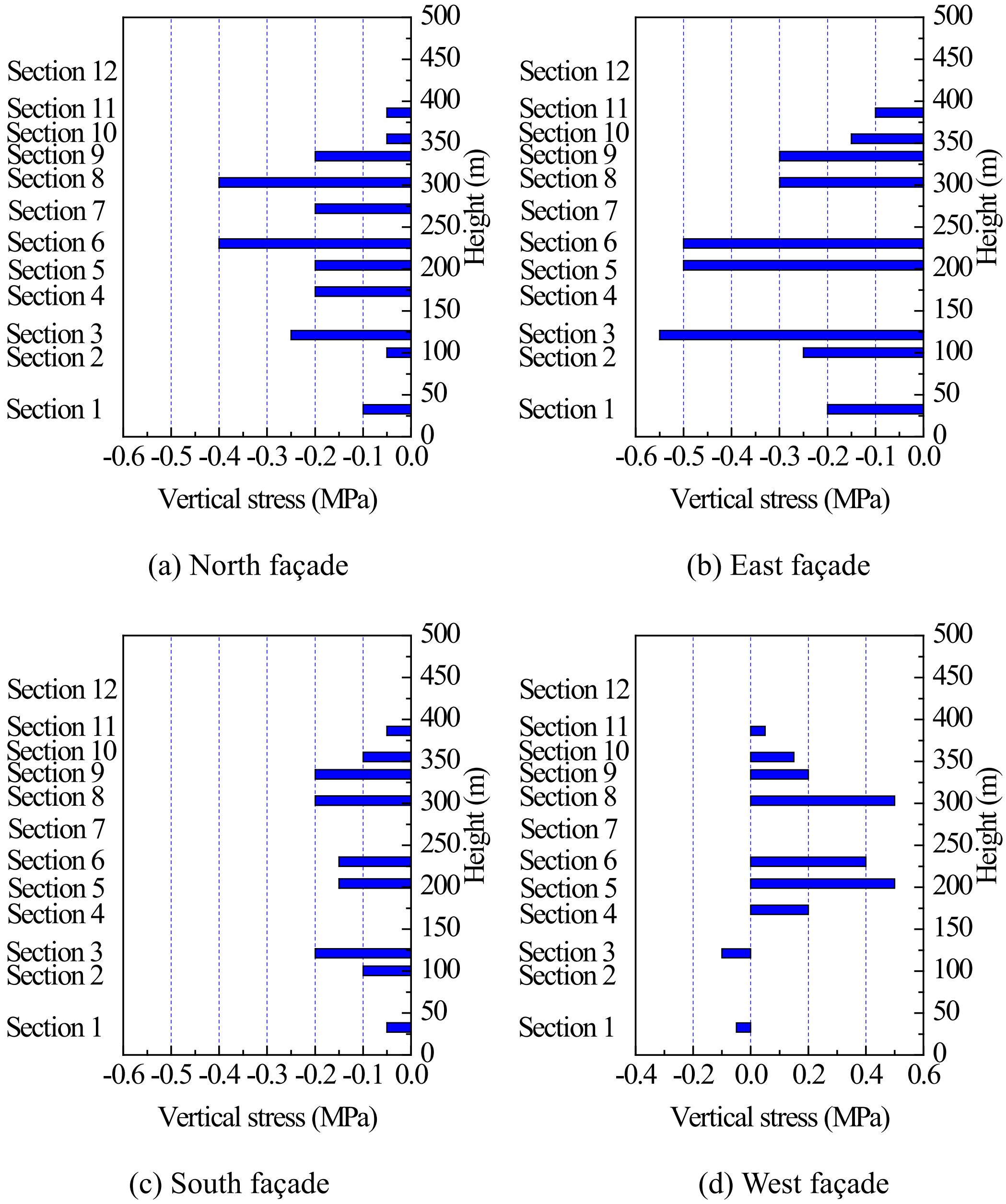

Figure 8. Maximum vertical stress along the structural height during the typhoon period

Strain sensors on the outer tube were lost in September 2013 because of the data acquisition system was shut down during this month. The typhoon-induced stress for the outer tube was not measured.

The wind speed from 0:00 to 24:00 on 21 September was low. The structural responses could be treated as temperature loading effects only. From 2:00 on 22 to 8:00 on 23 September, the wind was strong and temperature variation was significant. Consequently the structural responses were caused by the combined loading effects. The typhoon-induced quasi-static responses could be separated from the total responses by calculating the temperature-induced responses using FE analysis.

4. Separation of Typhoon- and Temperature-induced Quasi-static Responses through Structural Analysis

4.1. Temperature loading model of Canton Tower

To calculate the temperature-induced responses with FE analysis, the temperature distribution of the structure measured from the field SHM system and the global FE model (Figure 1(d)) are employed. The measurement data on 21 September are initially used to verify the effectiveness of this numerical approach because the structural responses on that day are solely from temperature variations. Four temperature loading cases at different time instants are studied: 6:00 (Case 1), 10:00 (Case 2), 17:30 (Case 3), and 24:00 (Case 4) on 21 September. The temperature distribution of the entire structure at 9:00 on 23 September is selected as the reference state (Case 0) because the measurement data indicate that the temperature distribution at this instant is relatively uniform. The measured temperatures of the structural components in the four loading cases are imported to the FE model, and their difference relative to that of Case 0 are regarded as the temperature loading. The calculated displacement and stresses are responses induced by temperature loading only.

The number of the field measurement points is generally smaller than the number of nodes in the numerical FE model. In the case, an appropriate temperature loading model is required. Su et al. (2016) used the monitoring data of Canton Tower for seven years (from 2008 to 2014) to study the temperature distribution of the structure. It was found that the tower exhibits a significant temperature difference between its inner and outer tubes as well as among the façades. A temperature loading model was proposed on the basis of the measurement data and numerical heat-transfer analysis. The global temperature distribution of the FE model is then simplified as follows:

(i). The components on the same façade are assumed to have similar temperature at one time instant.

(ii). The temperature of the floor slab is assumed equal to the mean temperature of the inner tube because the floor slabs are enclosed by a curtain wall and an inner wall.

(iii). The differences between inner and outer tubes are simplified as the differences between the mean temperature of the inner wall and that of the four outer columns where temperature sensors are installed.

4.2. Temperature-induced quasi-static responses calculated from structural analysis

The temperature-induced responses are calculated with the temperature loading in each loading case. Figure 9 compares the calculated and measured horizontal displacement of the tower top (465 m) in all cases on 21 September. The origin denotes Case 0 and the displacement at other time instants is relative to Case 0. The calculated horizontal displacement agrees well with the field measurement in all time instants. This verifies that simplified temperature model is effective for obtaining the temperature-induced displacement of the structure.

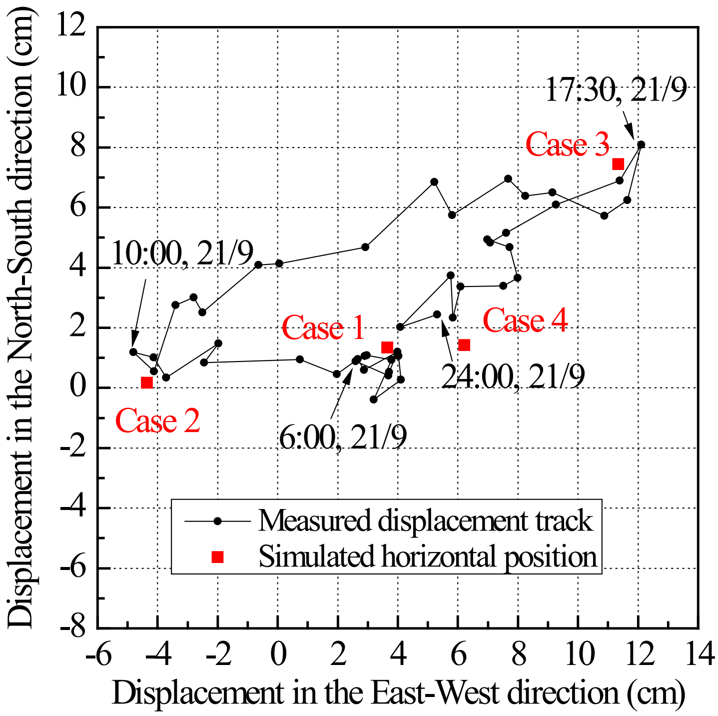

Figure 9. Comparison between the calculated and measured horizontal displacement at the tower top

The temperature-induced vertical stresses of the west façade of the inner tube in all four cases are plotted in Figure 10, in which the field measurement results are compared with the calculated ones. Both the simulated and measured stresses along the height of the tower are generally in agreement, although discrepancy can be found in the segments where the inner tube connects with functional floors. This discrepancy may be attributed to the inaccuracy of the temperature data used in the simplified FE model. For example, the temperature distribution of the floor slabs is assumed uniform as no sensor has been installed on the floors. Another possible reason is measurement noise. The largest temperature-induced vertical stress is approximately 0.8 MPa, which is at Section 8 (303.2 m high).

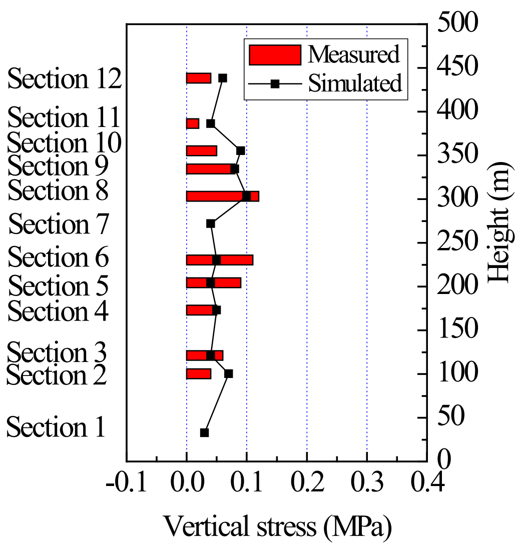

(a) Case 1

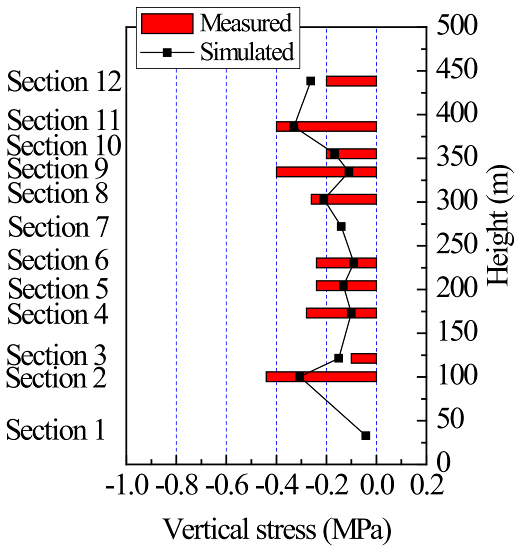

(b) Case 2

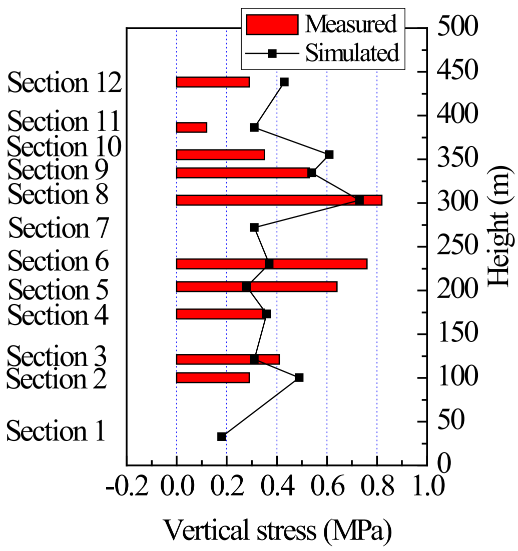

(a) Case 3

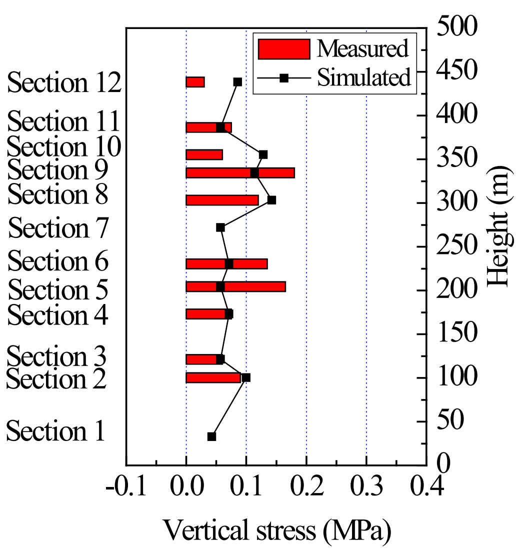

(b) Case 4

Figure 10. Temperature-induced stress of the west façade of the inner tube

4.3. Typhoon-induced quasi-static responses

The temperature-induced quasi-static responses of the structure can be calculated effectively from the measured temperature data and FE model. The same approach is applied to calculate the temperature-induced quasi-static responses during the typhoon period. Seven other time instants during the typhoon period on 22-23 September (Table I) are studied. The temperatures at these instants are inputted into the FE model. The calculated structural responses are regarded as induced by temperature loading solely. Structural displacement and stresses induced by the typhoon only are then determined by subtracting the temperature-induced responses from the measured total responses.

Table I. Calculated horizontal displacement at the tower top (465 m) induced by temperature variation

Time instant		Horizontal displacement (cm)	
		East-west	North-south
1	14:00, 22 Sept.	5.0	1.7
2	18:00, 22 Sept.	2.0	1.5
3	22:00, 22 Sept.	0.3	1.3
4	02:00, 23 Sept.	−1.0	1.6
5	04:00, 23 Sept.	−1.2	1.1
6	05:30, 23 Sept.	−1.1	0.5
7	08:00, 23 Sept.	−1.5	−0.1

The temperature-induced horizontal displacement at the tower top in these cases is listed in Table I. The corresponding horizontal quasi-static displacement induced by the typhoon only is then calculated and illustrated in Figure 11. The maximum east-west displacement is 11.2 cm, occurring at 4:00 on 23 September, whereas the maximum south-north displacement is 4.9 cm, occurring at 2:00 on the same day. The peak-to-peak horizontal displacement induced by the typhoon is 13.1 and 7.1 cm in the east-west and south-north direction, respectively. The values are larger than those under the combined loading effects (10.1 and 7.0 cm in the east-west and south-north direction, respectively, as shown in Figure 6). If the thermal effects are not removed, the typhoon-induced displacement will be underestimated. Nevertheless, the typhoon-induced displacement is smaller than the temperature-induced displacement in a typical sunny day (peak-to-peak displacement of 17.8 and 8.5 cm in the east-west and south-north direction, respectively). The calculated wind-induced displacement will be compared with the wind tunnel test results in the next section.

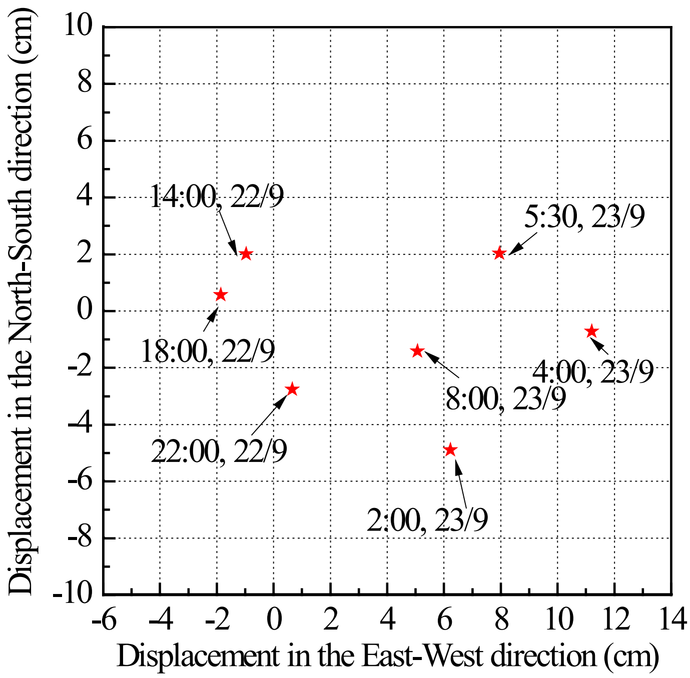

Figure 11. Calculated horizontal displacement at the tower top caused by Typhoon Usagi

Table II. Calculated stresses at an elevation of 303.2 m induced by temperature variation and typhoon

Time instant		Temperature-induced stress (MPa)				Typhoon-induced stress (MPa)			
		North	East	South	West	North	East	South	West
1	14:00, 22 Sept.	0.02	0.02	−0.02	0.02	0.03	0.02	0.02	0
2	18:00, 22 Sept.	0.01	0.01	0	−0.01	0.01	0.04	0.03	0.01
3	22:00, 22 Sept.	−0.02	−0.02	−0.02	−0.03	−0.06	0.06	0.02	0.06
4	2:00, 23 Sept.	−0.06	−0.08	−0.07	−0.13	−0.28	−0.16	−0.01	0.59
5	4:00, 23 Sept.	−0.10	−0.14	−0.14	−0.26	−0.30	−0.16	−0.06	0.76
6	5:30, 23 Sept.	−0.09	−0.16	−0.15	−0.29	−0.25	−0.13	−0.01	0.51
7	8:00, 23 Sept.	−0.05	−0.11	−0.09	−0.16	−0.12	−0.06	−0.01	0.32

The temperature-induced stresses at the elevation of 303.2 m in these different cases are calculated and listed in Table II. The typhoon-induced stresses after removing the thermal effect are also listed. The calculated stress variations of north, east, south, and west façades at the specified elevation at 4:00 on 23 September are approximately −0.10, −0.14, −0.14, and −0.26 MPa, respectively. After eliminating the thermal effect, the typhoon-induced quasi-static stresses of the four façades are approximately −0.30, −0.16, −0.06, and 0.76 MPa, which are comparable to the stresses caused by daily temperature variation. The largest variation in stress induced by the typhoon was roughly 0.76 MPa, accounting for 8% of the total stress approximately.

5. Wind Tunnel Test of Aeroelastic Model of Canton Tower

5.1 Description of the wind tunnel test

An aeroelastic model of the full tower was tested [21] in the TJ-2 Boundary Layer Wind Tunnel at Tongji University (Figure 12). The testing section of the wind tunnel is 3 m wide, 2.5 m high, and 15 m long.

The geometric length scale of the model (λ_L) is 1:266, according to the dimensions of the wind tunnel and the tower model. The simulation of Froude Number was ignored in this test because of the negligible effect of gravity on the structural stiffness of the tower. The frequency scale (λ_f) is 47:1. The air in the wind tunnel is identical to that in situ; thus, the air density scale (λ_ρ) is 1:1. Other scales are derived from the three basic scales (i.e., λ_L, λ_f, and λ_ρ) through the dimensional analysis.

The model was firmly placed at the center of a 2.8 m diameter rotatable plate. The surrounding buildings up to a distance of 500 m were represented by plastic plates at the same geometric scale. Laser displacement sensors were mounted at heights of 278, 355, and 443 m to measure the horizontal displacements in east and north directions and the twist around the vertical axis, respectively. The frequencies of the first two bending mode shapes of the scaled model were f_1=4.461 Hz, f_2=6.525 Hz. Zhu et al. [21] reported the details of the wind tunnel test.

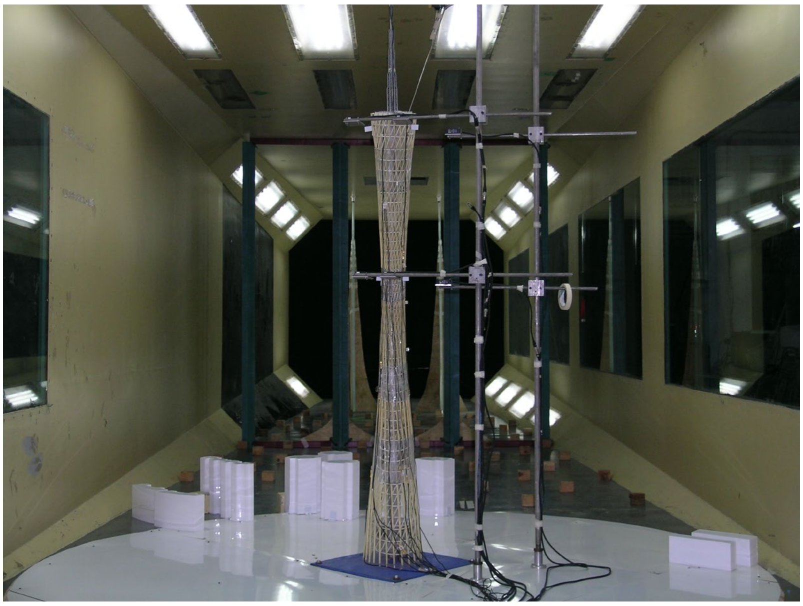

Figure 12. Aeroelastic model of the full tower in the TJ-2 wind tunnel

5.2 Wind-induced displacement responses

The wind tunnel test of the aeroelastic model was carried out for 32 different wind directions ranging from 0° (due north) to 360° clockwise at 11.25° intervals by rotating the base plate accordingly (Figure 13). In each wind direction, the responses of the model were measured under wind speeds ranging from 0 to 11 m/s, corresponding to the prototype wind speed of 0 to 62.3 m/s. No vortex-excited resonance phenomenon was observed; hence, the simulated results focus on the stochastic vibration responses of the tower to the wind [21].

The mean horizontal displacement in the wind tunnel test is compared with the field measurement. The wind tunnel test results are transferred to the prototype results. The field measurement results caused by the typhoon only are obtained by eliminating the temperature effect, as detailed in Section 4.3. Two wind direction cases corresponding to the maximum horizontal displacement in Typhoon Usagi are presented for comparison. During the typhoon, the largest horizontal displacement in the east-west direction was approximately 11.2 cm from the reference position (Figure 11), occurring at 4:00 on 23 September when mean wind speed was 25 m/s and wind direction was 285°. Figure 14(a) shows the horizontal displacement versus different mean wind speed in the wind tunnel test when the wind direction was 281.25°.

The displacement at the mean wind speed of 25 m/s was 12.0 cm, very close to the measurement result. The largest horizontal displacement in the south-north direction was roughly −4.9 cm, occurring at 2:00 on 23 September, when the mean wind speed was 23 m/s and wind direction was 320°. The corresponding displacement in the wind tunnel test was −2.3 cm when the wind direction was 315° (Figure 14(b)). Both subplots show that the horizontal displacements vary approximately in a quadric relation with the mean wind speed.

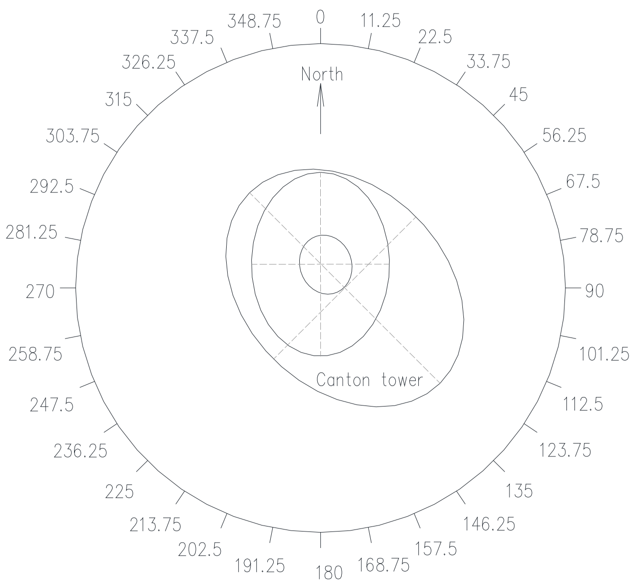

Figure 13. Coordinate system of the tower and 32 wind directions

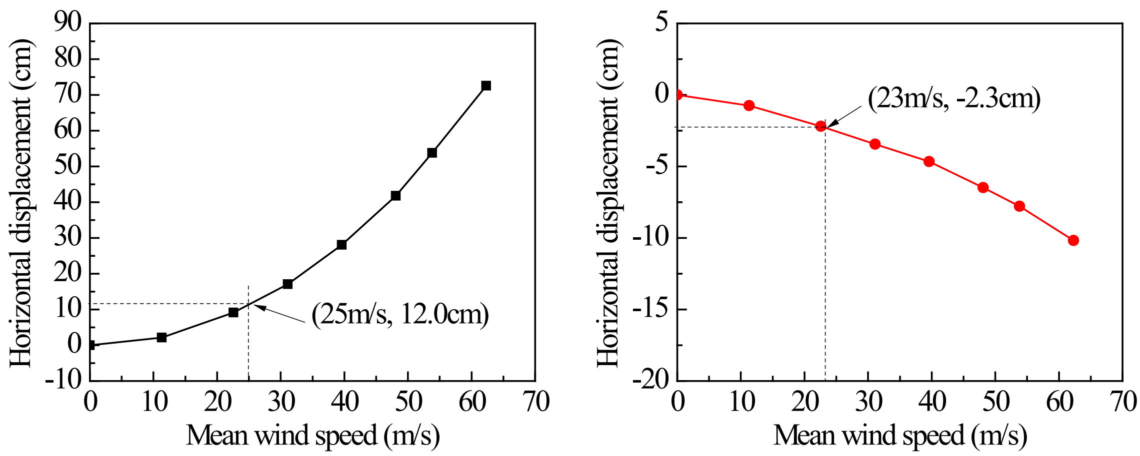

(a) East-west displacement (wind direction of 281.25°)

(b) South-north displacement (wind direction of 315°)

Figure 14. Quasi-static horizontal displacement at 443 m in the wind tunnel test

6. Conclusions

Appropriate separation of the temperature and wind loading effects is important to obtain the wind-induced quasi-static responses during a typhoon because the air temperature tends to decrease during the typhoon period and the thermal effect on the structure is significant. The temperature loading effect is separated using the temperature distribution model of Canton Tower. The calculated temperature-induced horizontal displacement and stresses agree well with the field measurements. The simplified temperature model is effective in obtaining the temperature-induced responses of the entire structure.

After eliminating the temperature effect, the peak-to-peak horizontal mean displacement at the tower top induced by the strong Typhoon Usagi is 13.1 and 7.1 cm in the east-west and south-north direction, which are larger than the combined displacement due to mean wind and temperature (10.1 and 7.0 cm). This indicates that using the combined loading effect may underestimate the mean wind loading alone. Moreover, the mean wind induced displacements are smaller than those caused by the temperature variation in a typical sunny day (17.8 and 8.5 cm). The maximum stress of the inner tube caused by the typhoon is roughly 8% of the total stress of the structure. The measured wind-induced quasi-static displacement agrees with the results of the wind tunnel test using an aeroelastic model of the tower.

The typhoon-induced quasi-static responses of Canton Tower are not very significant as compared with the total height of the structure, possibly because of the lattice-formed outer tube. Although the response magnitude of the present structure does not represent other supertall structures, the separation method proposed in this study can be applied to other structures.

Acknowledgments

This research was supported by the Research Grants Council of the Hong Kong Special Administrative Region, China (Project No. PolyU 152621/16E), NSFC Joint Research Fund for Overseas and Hong Kong and Macao Scholars (Project No. 51629801), and Research Grant of the Fuzhou University (Project No. 510251) and the Education Department of Fujian Province (Project No. 601705).

References

[1] Boggs DW, Peterka J. Aerodynamic model tests of tall buildings. J Eng Mech 1989; 115(3): 618–635.

[2] Fediw AA, Nakayama M, Cooper KR, Sasaki Y, Resende IS, Zan SJ. Wind tunnel study of an oscillating tall building. J Wind Eng Ind Aerod 1995; 57: 249–260.

[3] Kareem A. Dynamic response of high-rise buildings to stochastic wind loads. J Wind Eng Ind Aerod 1992; 42: 1102–1112.

[4] Zhou Y, Kareem A, Gu M. Equivalent static buffeting wind loads on structures. J Struct Eng 2000; 126: 989–992.

[5] Gu M, Quan Y. Across-wind loads of typical tall buildings. J Wind Eng Ind Aerod 2004; 92(13): 1147–1165.

[6] Quan Y, Gu M, Tamura Y. Experimental evaluation of aerodynamic damping of square super high-rise buildings. Wind Struct 2005; 8(5): 309–324.

[7] Kim YM, You KP, Ko NH. Across-wind responses of an aeroelastic tapered tall building. J Wind Eng Ind Aerod 2008; 96(8): 1307–1319.

[8] Kim Y, Kanda J. Characteristics of aerodynamic forces and pressures on square plan buildings with height variations. J Wind Eng Ind Aerod 2010; 98(8): 449–465.

[9] Brownjohn JMW, Pan TC. Identifying loading and response mechanisms from ten years of performance monitoring of a tall building. J Perform of Constr Fac 2008; 22(1): 24–34.

[10] Kijewski-Correa T, Kilpatrick J, Kareem A, Kwon DK, Bashor R, Kochly M, Young BS, Abdelrazaq A, Galsworthy J, Isyumov N, Morrish D, Sinn RC, Baker WF. Validating wind-induced response of tall buildings: synopsis of the Chicago full-scale monitoring program. J Struct Eng 2006; 132(10): 1509–1523.

[11] Yi TH, Li HN, Gu M. Recent research and applications of GPS-based monitoring technology for high-rise structures. Struct Control Hlth 2013; 20(5): 649–670.

[12] Park HS, Shon HG, Kim IS, Park JH. Application of GPS to monitoring of wind-induced responses of high-rise buildings. Struct Des Tall Spec 2008; 17(1): 117–32.

[13] Xia Y, Zhang P, Ni YQ, Zhu HP. Deformation monitoring of a super-tall structure using real-time strain data. Eng Struct 2014; 67: 29-38.

[14] Xia Y, Chen B, Zhou XQ, Xu YL. Field Monitoring and Numerical Analysis of Tsing Ma Suspension Bridge Temperature Behavior. Struct Control Hlth 2013; 20(4): 560–575.

[15] Zhou LR, Xia Y, Brownjohn JMW, Koo YK. Temperature Analysis of a Long-span Suspension Bridge based on Field Monitoring and Numerical Simulation. J Bridge Eng 2016; 21(1): 04015027.

[16] Pirner M, Fischer O. Long-time observation of wind and temperature effects on TV towers. J Wind Eng Ind Aerod 1999; 79(1-2): 1–9.

[17] Breuer P, Chmielewski T, Gorski P, Konopka E, Tarczynski L. The Stuttgart TV Tower-displacement of the top caused by the effects of sun and wind. Eng Struct 2008; 30(10): 2771–2781.

[18] Tamura Y, Matsui M, Pagnini LC, Ishibashi R, Yoshida A. Measurement of wind-induced

response of buildings using RTK-GPS. J Wind Eng Ind Aerod 2002; 90(12–15): 1783–1793.
[19] Azkune M, Puente I, Insausti A. Effect of ambient temperature on the redistribution of loads during construction of multi-storey concrete structures. Eng Struct 2007; 29(6): 933–941.
[20] Li DS, Ren L, Li HN, Song GB. Structural health monitoring of a tall building during construction with fiber bragg grating sensors. Int J Distrib Sens N 2012; 2012: 1–10.
[21] Zhu LD, Ding QS, Tan X, Wen SB. Aeroelastic model test of a 610m-high TV Tower in Guangzhou City of China. Proceedings of the 12th International Conference on Wind Engineering, Cairns, Australia, 2007; 1: 975–982.
[22] Ni YQ, Xia Y, Liao WY, Ko JM. Technology innovation in developing the structural health monitoring system for Guangzhou New TV Tower. Struct Control Hlth 2009; 16(1): 73–98.
[23] Su JZ, Xia Y, Ni YQ, Zhou LR, Su C. Field monitoring and numerical simulation of the thermal actions of a supertall structure. Struct Control Hlth 2016. (Accepted)
[24] CEB-FIP. Model Code 1990. London: Thomas Telford; 1993.
[25] Xia Y, Xu YL, Wei ZL, Zhu HP, Zhou XQ. Variation of structural vibration characteristics versus non-uniform temperature distribution. Eng Struct 2011; 33: 146–153.
[26] Xia Y, Ni YQ, Zhang P, Liao WY, Ko, JM. Stress development of a super-tall structure during construction: field monitoring and numerical analysis. Comput-Aided Civ Inf 2011; 26(7): 542–559.
[27] SAP2000. SAP2000 Linear and Nonlinear Static and Dynamic Analysis and Design of Three-Dimensional Structures. Berkeley, California, USA, version 14.0, Computers and Structures Inc.; 2009.
[28] Chen WH, Lu ZR, Lin W, Chen SH, Ni YQ, Xia Y, Liao WY. Theoretical and experimental modal analysis of the Guangzhou New TV Tower. Eng Struct 2011; 33(12): 3628-3646.